Available online at www.sciencedirect.com
SCIENCE DIRECT®
Physica A 333 (2004) 225–240
PHYSICA A
www.elsevier.com/locate/physa

Two-regime dynamical behaviour in Lennard–Jones systems: Spectral and rescaled range analysis

T.E. Karakasidis*, A.B. Liakopoulos

Hydromechanics Laboratory, Department of Civil Engineering, School of Engineering, University of Thessaly, Volos 38334, Greece

Received 11 March 2003; received in revised form 26 August 2003

Abstract

In this work we present an analysis of temperature and pressure time series obtained by microcanonical (constant energy) molecular dynamics simulations. Simulations in the solid and fluid states were performed using a Lennard–Jones potential to describe atomic interactions. Several points of the system density–temperature phase diagram have been investigated for reduced densities ρ^* in the range [0.2–1.4] and reduced temperatures T^* in the range [1.5–2.5]. Power spectral analysis shows evidence of a two-regime power-law $1/f^a$ behaviour with a large exponent at the high-frequency region and a smaller exponent at low frequencies. Rescaled range analysis (Hurst test) also reveals a two-regime behaviour. The exponent a depends on the system density and temperature. All time series exhibit essentially the same characteristics for short times (large frequencies). In contrast, at low frequencies, pressure is characterized by a faster loss of memory. The relation of the computed time series behaviour to the physical characteristics of the system (such as particle mean square displacement and characteristic times) is discussed.

PACS: 02.70.Ns; 05.20.−y; 05.40.+j

Keywords: Molecular dynamics simulation; Lennard–Jones potential; Rescaled range analysis; Hurst test

* Corresponding author. Tel.: +30-24210-74054; fax: +30-24210-74054.
E-mail address: thkarak@uth.gr (T.E. Karakasidis).

0378-4371/$ - see front matter © 2003 Elsevier B.V. All rights reserved.
doi:10.1016/j.physa.2003.11.001

1. Introduction

Molecular dynamics (MD) is a widely used method for simulating materials at the atomic level. The equations of motion are solved and successive states of the system in the phase space are generated. During MD simulations several physical quantities of interest, such as temperature, potential energy, pressure, etc., can be followed in time giving rise to a number of time series that capture the dynamical characteristics of the system at the atomic level.

There is considerable interest in examining the underlying dynamical features of a variety of physical systems, which present similarities with features observed in well-documented dynamical systems, such as self-organized criticality. In a recent MD simulation of plastocyanin and surrounding water solvent [1] and in simulations of metal clusters [2] the occurrence of $1/f^a$ noise was found in the potential energy time series. Karakasidis and Andreadis [3] studied the instantaneous temperature and pressure time series generated during constant energy MD simulation of a grain boundary of nickel oxide and found that they exhibit $1/f^a$ behaviour. $1/f$ noise is also found in other physical systems [4–8] and in econometric time series (see for example Refs. [9,10]). In general, the occurrence of $1/f^a$ noise is considered as an indication of system complexity, $a = 1$ being the most commonly encountered case in the literature [7,11].

Lennard–Jones (LJ) potential has extensively been used in simulations of fluids and solids (see for example Refs. [12–15]). It is a simple model that is easily employed in MD simulations, permits fast calculations and is used in model calculation of large systems (see for example Refs. [16,17]). It is also an interaction potential for which many properties have been studied by MD computer simulation. We employed such a potential to describe the interaction of a model system in representative fluid and solid states. Our aim was to investigate if any frequency/time characteristics of the system dynamics could be revealed by the use of time-series analysis of microscopic and/or macroscopic quantities. In fact we performed an analysis of instantaneous temperature, potential energy and pressure generated by constant energy molecular dynamics simulation as the system (average) temperature and density are varied. The results presented here correspond to a series of simulations for reduced density ρ^* from 0.2 to 1.4 and reduced temperature T^* ranging from 1.5 to 2.5.

Power spectrum analysis reveals that all physical quantities exhibit a two-regime $1/f^a$ power-law behaviour with small exponents a for low frequencies and larger values for high frequencies. Rescaled range analysis (Hurst test) also confirms the presence of a two-regime behaviour with strong memory effects at small times (high frequencies) and weaker memory effects at large times (low frequencies). Further results on mean square displacements and characteristic times are found to be in agreement with the results from the spectral and Hurst analyses. The physical origin of this behaviour is discussed.

The paper is organized as follows: in Section 2 we give a brief description of the molecular dynamics simulation parameters and computational details. In Section 3 we present results of the analysis of the obtained time series and attempt the physical explanation of the system's dynamical features. Finally the conclusions are presented in Section 4.

2. Molecular dynamics simulation and computational details

The Lennard–Jones (12–6) potential

$$\varphi(r_{ij}) = 4\varepsilon \left[\left(\frac{\sigma}{r_{ij}} \right)^{12} - \left(\frac{\sigma}{r_{ij}} \right)^{6} \right] , \tag{1}$$

where r_{ij} denotes the distance between atoms i and j is used throughout this work and the cut-off distance for the interactions was set to 2.5σ. For argon the values of the parameters are $\sigma = 3.408$ Å and $\varepsilon/k_B = 119.8$ K, k_B being the Boltzmann constant. In reduced physical quantities Lennard–Jones units are used for which ε, σ and m act as units for energy, length and mass.

The simulated system contains 256 atoms. In order to start the simulation, atoms are located on an FCC lattice in a cube with edges parallel to the directions x:[100], y:[010] and z:[001]. The dimensions of the computational cell are such that we match the simulated reduced density of the system. Periodic boundary conditions were applied in the three directions x, y, z. Simulations were performed in the microcanonical (NVE) ensemble. The equations of motion were integrated using Verlet's algorithm [12], which is accurate and robust. To start the simulation, atoms are given appropriate velocities in order to reach the desired temperature conditions. Equilibration runs of 3×10^4 steps were performed before starting production runs.

We report here on MD simulations at reduced densities $\rho^* = 0.2$–0.8 (which correspond to fluid states) and $\rho^* = 1.2$, 1.4 (which correspond to solid states). At each density the system was simulated at five temperatures $T^* = 1.5$, 1.73, 2.0, 2.2, 2.5. All temperatures correspond to states above the critical point. At each state we performed ten independent production runs. Each production run was 10^{-10} s long and all relevant quantities were saved every 10^{-14} s. We focus our attention on the analysis of three time series:

Temperature,

$$T = \frac{1}{3Nk_B} \sum_{i=1}^{N} m_i \vec{v}_i^{\,2} , \tag{2}$$

potential energy,

$$U = \sum_{i=1}^{N} \sum_{j>i}^{N} \phi(r_{ij}) \tag{3}$$

and pressure

$$P = \frac{N}{V} k_B T - \frac{1}{3V} \sum_{i=1}^{N} \sum_{j>i}^{N} r_{ij} \frac{\partial \phi(r_{ij})}{\partial r_{ij}} , \tag{4}$$

where, as before, r_{ij} stands for the distance between two particles i and j, and $\vec{v}_i$ denotes the velocity of particle i. Further details can be found in Ref. [18].

3. Results and discussion

The representative time series for the instantaneous temperature and pressure are presented in Figs. 1(a)–(b), respectively, for a system (average) temperature $T^* = 1.5$ and $\rho^* = 0.2$.

3.1. Power spectra

In this work we calculate the power spectrum $P(f)$ of a time series x_j, $j = 1, 2, \ldots, N$ by applying the discrete Fourier transform [19] and setting

$$P(f) = N\|A(f)\|^2 , \tag{5}$$

where $\|A(f)\|$ denotes the modulus of

$$A(f) = \frac{1}{N}\sum_{j=1}^{N} x_j e^{i2\pi f j/N} . \tag{6}$$

In Fig. 2 we present the computed power spectra of the instantaneous temperature time series at several system states. At each state, the results are averaged over ten independent production runs performed with different initial conditions. We observe a two-regime power-law behaviour ($1/f^a$) in all cases. At high frequencies (small time intervals) we have a large value of the exponent a and at low frequencies (large time intervals) we have an exponent which appears to be significantly smaller. The exponents have been calculated by least-square fits both for the low-frequency and the high-frequency range. The least-square fitting was made for frequencies up to 1×10^{12} Hz for the low-frequency region, and from 5×10^{12} Hz to the highest frequency for the high-frequency region. For the solid, the high-frequency region begins at 8×10^{12} Hz. The computed values of the power spectrum exponent a are summarized in Fig. 3 and their trends are discussed below.

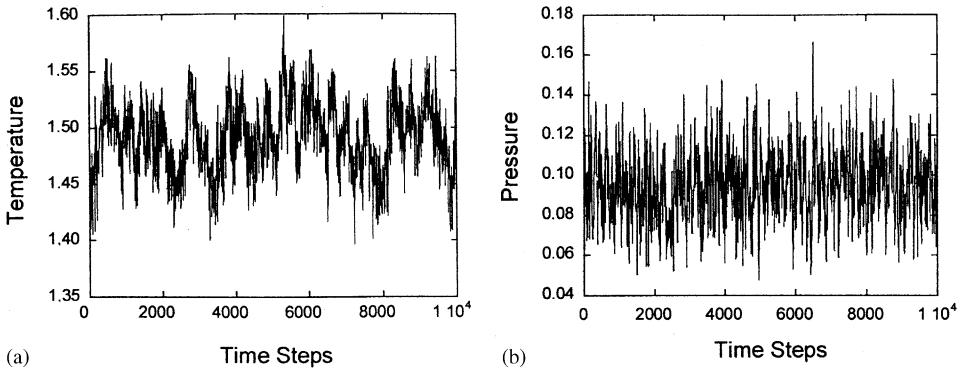

Fig. 1. Time series emanating from MD simulations at system (average) temperature $T^* = 1.5$ and $\rho^* = 0.2$. (a) instantaneous temperature, (b) instantaneous pressure.

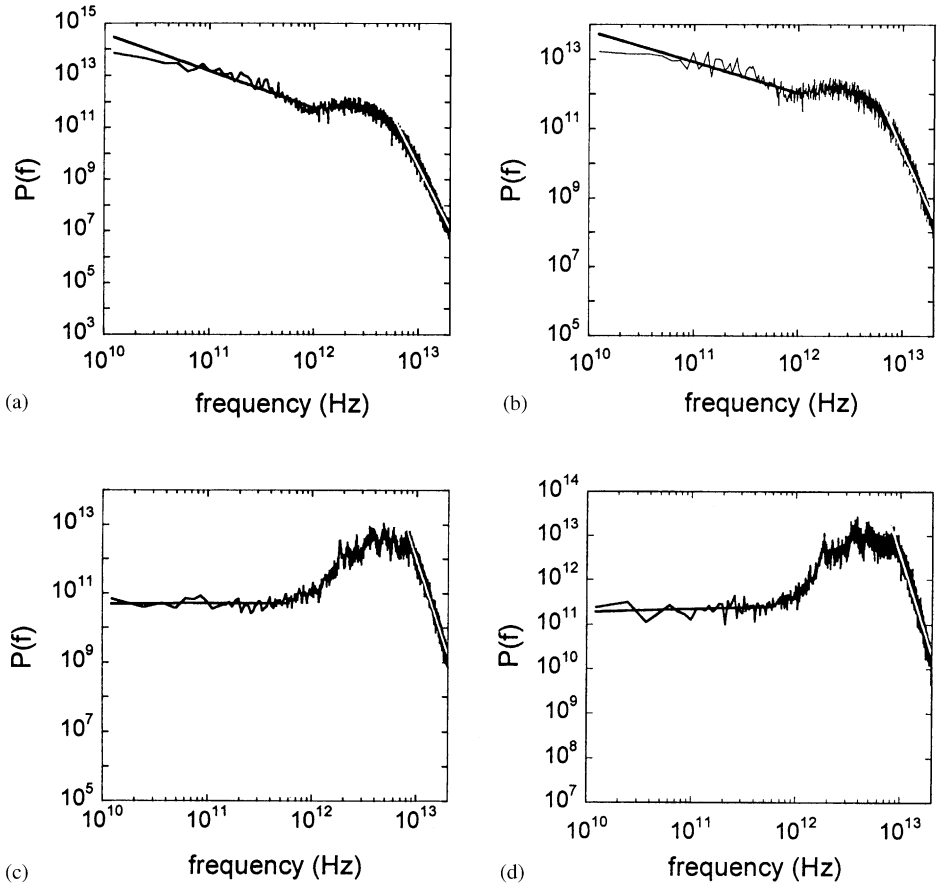

Fig. 2. Instantaneous temperature power spectra for the fluid states: (a) $\rho^* = 0.2$, $T^* = 1.5$, (b) $\rho^* = 0.2$, $T^* = 2.5$, and for the solid states (c) $\rho^* = 1.4$, $T^* = 1.5$, (d) $\rho^* = 1.4$, $T^* = 2.5$.

The low-frequency region exponents decrease as the density of the simulated fluid system increases. For the highest density they become comparable to those of the solid, which take values close to zero. We note here that $1/f^a$ behaviour is indicative of memory effects; the higher the exponent the stronger the effect. The value $a = 0$ corresponds to white noise i.e., a signal with no memory. The observed decrease in the value of the exponent a is indicative of the gradual loss of memory i.e., the new signal values depend less on their previous ones for large time intervals. The exponent values for the solid states are small and one could say that a white noise behaviour is approached in these states, i.e., fast loss of memory occurs.

The high-frequency region exponents of the fluid states, on the other hand, (Fig. 3(b)) seem to be insensitive to the value of the system density. Given that temperature depends on the atom velocities, this probably indicates that the dynamics

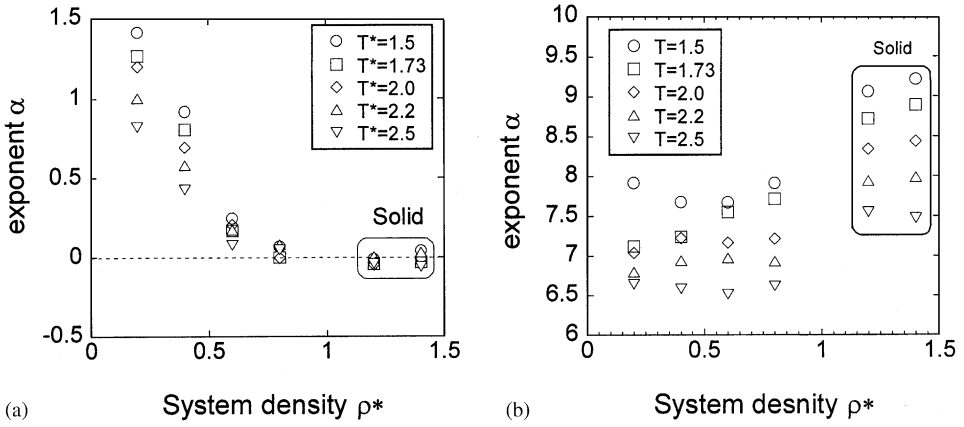

Fig. 3. Temperature power-spectrum *a* exponent as a function of system temperature and system density: (a) low-frequency domain, (b) high-frequency domain.

at short times is practically the same for all simulated densities of the fluid. The high values of the exponent indicate strong memory effects for short times, i.e., the new signal values depend strongly on the previous ones. In the case of a solid, the effect is stronger and this is indicated by the larger exponents.

System temperature also affects the values of the power-law exponents. In general, an increase in system temperature results in smaller exponents i.e., less pronounced memory effects. This trend is consistently evident in the high-frequency region but seems to hold for the low-frequency region too (compare Fig. 3(a) with (b)).

The physical origins of the above-described behaviour are discussed in the following paragraphs. We must bear in mind that temperature depends on the particle velocities (Eq. (2)) and thus on the dynamics of the system. In a dense fluid, atoms are packed rather closely together, and their motions cannot be as free as they are in a dilute fluid. In a dilute fluid atoms move around and during these motions they "collide" with each other. Such a "collision" leads to deviation of the atom from its straight path, so that its trajectory finally resembles a complicated pattern of broken lines. In a densely packed fluid, on the other hand, atoms are so confined by their neighbours that they can only vibrate as if inside a "cage". As soon as the atom moves away from the centre of the "cage", "collision" events with its neighbours reverse its velocity and send it back. These kinds of motions have relatively high frequencies of order 10^{12}–10^{13} Hz similar to those of the vibrational motion in a solid. However, the "cage" is not rigid as it consists of other atoms, which also undergo thermal motions. From time to time its neighbours move in such a collective way, that they let the central atom move outside the "cage" and start on a diffusive type of motion which will lead it away from its initial position. As a result atoms in a dense fluid are hopping along a zig-zag-type trajectory consisting of discrete jumps between sites of residence where the atoms vibrate (before jumping). The hopping frequencies are lower than the vibrational ones. As a result we have in the case of a fluid two kinds of frequencies,

low frequencies related to diffusive motion and higher frequencies related to vibrational motion. Rahman [20] who performed an early simulation of liquid argon at a given liquid state found that the velocity autocorrelation function ($VAF = \langle \vec{v}(0) \cdot \vec{v}(t) \rangle$) and its power spectrum, $F(\omega)$, presented characteristics related to these fluctuations of the structure of the "cages". In fact, Rahman found that $F(\omega)$ had a solid-like part and a diffusive part due to the particle's taking advantage of the local fluctuation in the configuration of its neighbours to move in the "easy" direction afforded to it by the fluctuations.

In the present work, for all system states studied, a two-regime behaviour is observed in the case of the temperature time series with an intermediate region of frequencies (10^{12}–5×10^{12} Hz). The high-frequency behaviour corresponds to short time dynamics. At small time intervals the particles move as free particles, and their new positions depend strongly on their previous ones. The same holds for their velocities and, as a result, this is reflected in the instantaneous temperature power spectrum through a large exponent a. The increase of temperature at a given density results in higher particle velocities and as a result atoms move faster, "collisions" occur more often and thus memory is lost faster. This faster loss of memory is reflected in the temperature and could explain the reduction in the value of the exponent a as the system temperature rises. On the other hand, the increase of the density (at a given temperature) does not result in any significant modification of the exponents this being indicative that the short time dynamics are practically the same for all fluid states. This is further confirmed by the results on means square displacement, MSD, presented in Section 3.3.

For low frequencies (large time intervals) in the case of fluid, the exponent a increases as the density decreases because we have a slower loss of memory due to the fact that "cages" become less rigid as the fluid becomes more dilute. In fact as the system density decreases (at a given temperature) collisions occur less often than in the case where atoms are more densely packed and thus at large time scales (low frequencies) there is a slower loss of memory. Temperature depends on the particle velocities and as a result a decrease in the a exponent of the power spectrum is observed. An increase in temperature (at given density) seems to lead to lower values of the exponent a since an increase in temperature results in larger velocities and thus a faster loss of memory.

In the case of the solid, atoms vibrate around their positions and do not diffuse, as is the case in the fluid phase. For very short times, atoms are accelerated up to the largest amplitude of vibration and then their velocities change sign, so their position and velocities are strongly correlated at short times (high frequencies) but their positions become uncorrelated rather quickly at large time intervals (small frequencies). The same behaviour holds for their velocities and this is reflected in the instantaneous temperature, which depends on instantaneous atomic velocities. As a result, we have large values of exponents a in the high-frequency region and small ones in the low-frequency region.

It is of interest to note that in the case of the solid we have characteristic vibration modes, phonons, which in the case of argon, for the studied system states, have frequencies that lie in the region 2–5 THz. Velocities will have characteristic frequencies in this interval too, and as a result temperature which depends on the velocities exhibits

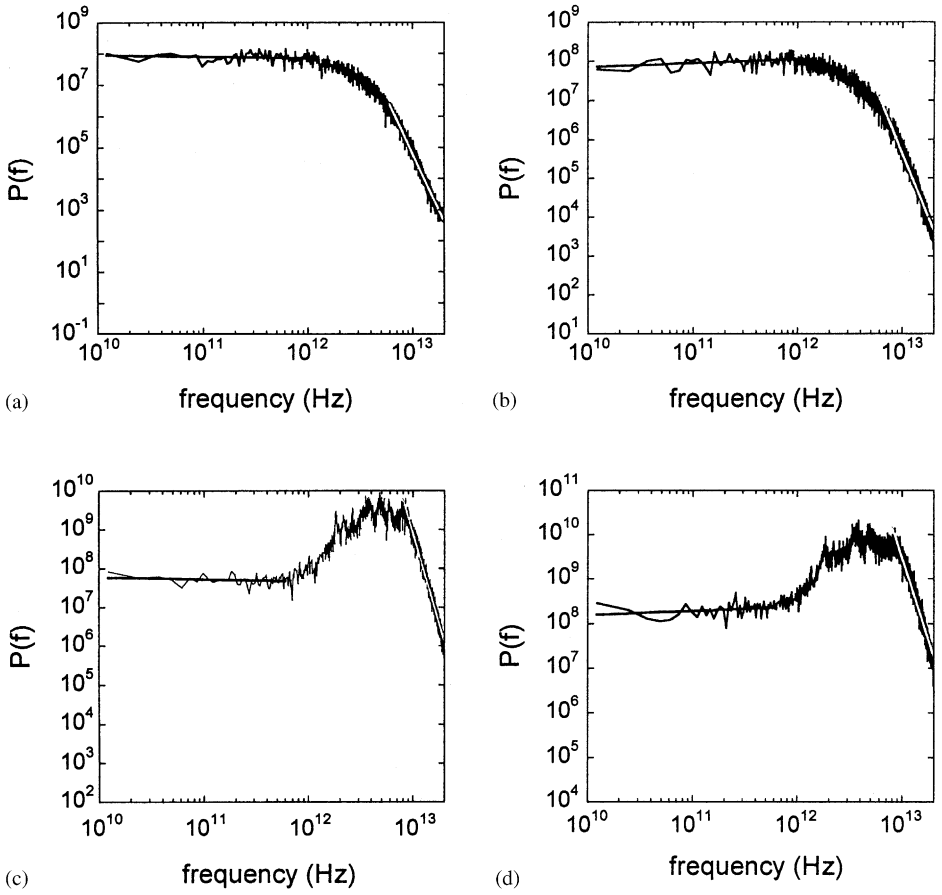

Fig. 4. Instantaneous pressure power spectra for the fluid states (a) $\rho^* = 0.2$, $T^* = 1.5$, (b) $\rho^* = 0.2$, $T^* = 2.5$, and for the solid states (c) $\rho^* = 1.4$, $T^* = 1.5$, (d) $\rho^* = 1.4$, $T^* = 2.5$.

a broad "peak" in the power spectrum around that frequency zone (see Figs. 2(c) and 2(d)). This behaviour of the temperature power spectrum seems to be distinctively different from that of the fluid where no such broad peak exists around this frequency interval.

Note that the potential energy power spectrum is identical to that of the kinetic energy (temperature) within numerical accuracy since in the microcanonical ensemble the sum of the kinetic energy (temperature) and of the potential energy is constant. For a thorough discussion of this point see Lebowitz et al. who have shown rigorously that the variances of the kinetic energy and potential energy are equal in the microcanonical ensemble [21].

Typical pressure power spectra are presented in Fig. 4. A two-regime power-law behaviour is again evident with a high slope at the high-frequency region and a

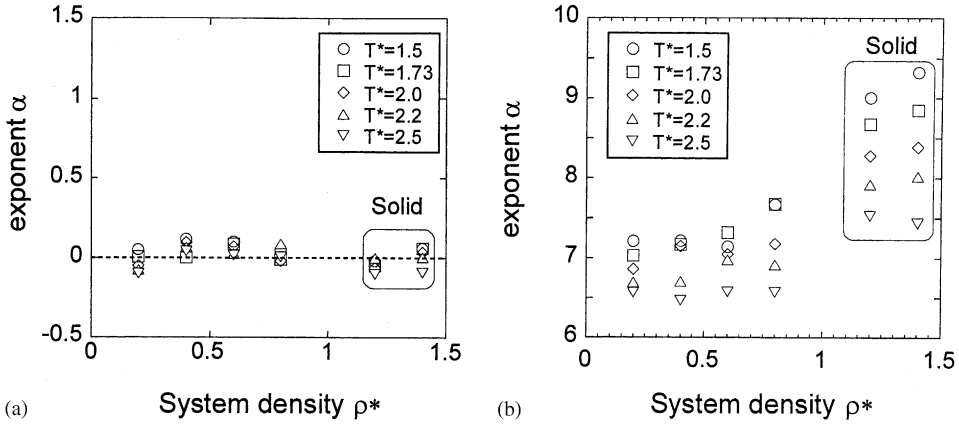

Fig. 5. Pressure power spectrum a exponent as a function of system temperature and system density (a) low-frequency domain, (b) high-frequency domain.

low-frequency region with a much smaller slope. The exponents for the two regions are plotted in Fig. 5. The exponents of the high-frequency region are quite similar to that of the temperature (and potential energy); however, the exponents for the low-frequency region are close to zero indicating almost white noise behaviour even for the fluid states. We think that this behaviour can be explained by examining Eq. (4). Pressure depends on temperature (i.e., velocities), and also on products of the form $r_{ij}(\partial\phi(r_{ij})/\partial r_{ij})$, i.e., the product of the distance with the force between two particles i, j. It seems that at short times (high frequencies) memory effects are present but they are almost completely lost at large times (small frequencies) probably due to the presence of this cross term.

3.2. Rescaled range analysis (Hurst test)

Rescaled range analysis (R/S) also known as Hurst test, [22,23], can be briefly described as follows: let us denote by $T(i)$, $i=1,\ldots,N$, the elements of a time series T. For every n, $2 \leqslant n \leqslant N$, we denote by $\langle T\rangle_n$ the mean value of the first n elements of the time series T, i.e.,

$$\langle T\rangle_n = \frac{1}{n}\sum_{j=1}^{n} T(j)\,. \tag{7}$$

Then, we compute $X_i(n)$, the accumulated deviation from the mean $\langle T\rangle_n$, with elements

$$X_i(n) = \sum_{k=1}^{i} [T(k) - \langle T\rangle_n], \quad i=1,2,\ldots,n\,. \tag{8}$$

The range of the accumulated deviation from the average level is the difference between the maximum and the minimum cumulative deviations over n periods and is denoted

by R_n, i.e.,

$$R_n = \max_{1 \leqslant j \leqslant n}(X_j(n)) - \min_{1 \leqslant j \leqslant n}(X_j(n)) \,. \tag{9}$$

The function R_n generally increases as a function of n. Let us also denote by S_n the standard deviation of the first n elements of the time series $\{T(j)\}$, i.e.,

$$S_n = \sqrt{\frac{1}{n}\sum_{k=1}^{n}[T(k) - \langle T\rangle_n]^2} \,. \tag{10}$$

In the case of a fractional Brownian motion in the limit of large n,

$$(R_n/S_n) \propto (n)^H \,, \tag{11}$$

with $0 \leqslant H \leqslant 1$, the Hurst exponent [23].

The method provides information on the persistent (long-range correlated), anti-persistent or pure random character of the time series $\{T(j)\ j = 1, 2, \ldots, N\}$. We can plot $\log(R_n/S_n)$ vs. $\log(n)$ and, in the case of scaling, we can estimate the value of the Hurst exponent which contains quantitative information. We remind the reader here that for time series with consecutive values generated by statistically independent processes with finite variances $H = 0.5$ (uncorrelated or white noise). The case $0.5 < H < 1$ corresponds to processes where fluctuations in subsequent values are positively correlated (persistence), while the case $0 < H < 0.5$ corresponds to processes where fluctuations in subsequent values are negatively correlated (anti-persistence) e.g. large positive values are followed by large negative values and vice versa.

In Fig. 6 we show the results of the R/S analysis of instantaneous temperature time series at several system states. At each system state results are averaged over ten independent production runs performed with different initial conditions. We observe a two-regime behaviour: a linear-type behaviour for small n (small time intervals) and a near linear behaviour with a smaller slope for higher n (large time intervals). We can in fact see that while at small n the linear approximation holds fairly well, at higher n we have some structures. One would be tempted to try to fit for selected intervals of n, but we think (see also Ref. [24]) that information on the global behaviour would be lost. So for the high n region we calculated the slope taking into account all data points for $\log n > 4.5$, and for small n the data for $\log n < 4.5$. It is worth noting that $\log n = 4.5$ corresponds approximately to a time interval of about 10^{-12} s and a frequency of about 10^{12} Hz which is the upper limit of the low-frequency region (see the power spectra in Figs. 2 and 4). The corresponding Hurst exponents for both regions (small and large n) for all simulated states are presented in Fig. 7.

In the fluid phase we observe that for small n (small time intervals/high frequencies) the values of H are close to unity indicating strong persistence, i.e., new values follow the trend of previous ones. This is in accordance with the results for the power spectrum analysis where a high slope a was found. For large n (large time intervals/small frequencies) the values of H are smaller and they decrease as the system density increases approaching the value of $H = 0.5$ (white noise) for the highest density studied. The decrease of H as density increases is in agreement with the results of the power spectrum analysis.

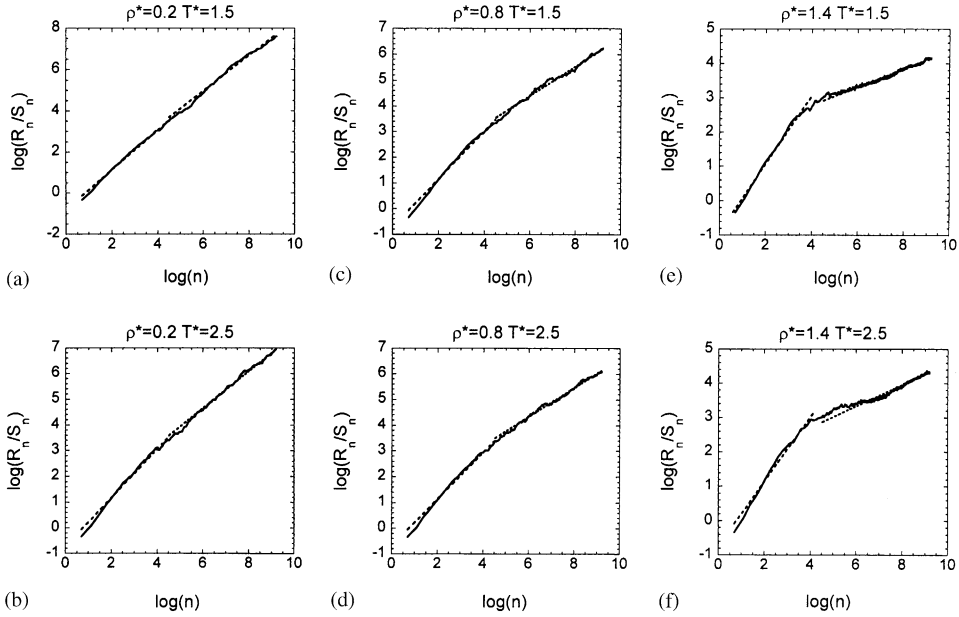

Fig. 6. Hurst test results for the temperature time series at various system densities ρ^* and temperatures T^*.

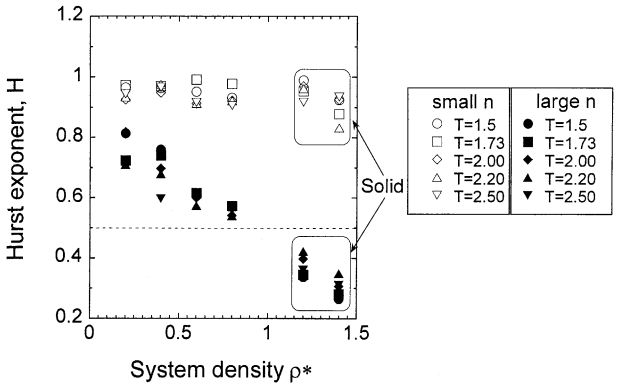

Fig. 7. Hurst exponents for the temperature time series as a function of system temperature and density.

In the solid phase, for small n (high frequencies) the exponents H exhibit a behaviour similar to that of the fluid, with values close to unity indicating strong persistence. This is in accordance with the results of spectral analysis which indicated strong memory effects. For large n (small frequencies) the exponents H are significantly smaller (around 0.3–0.5) indicating antipersistence. This behaviour is in agreement

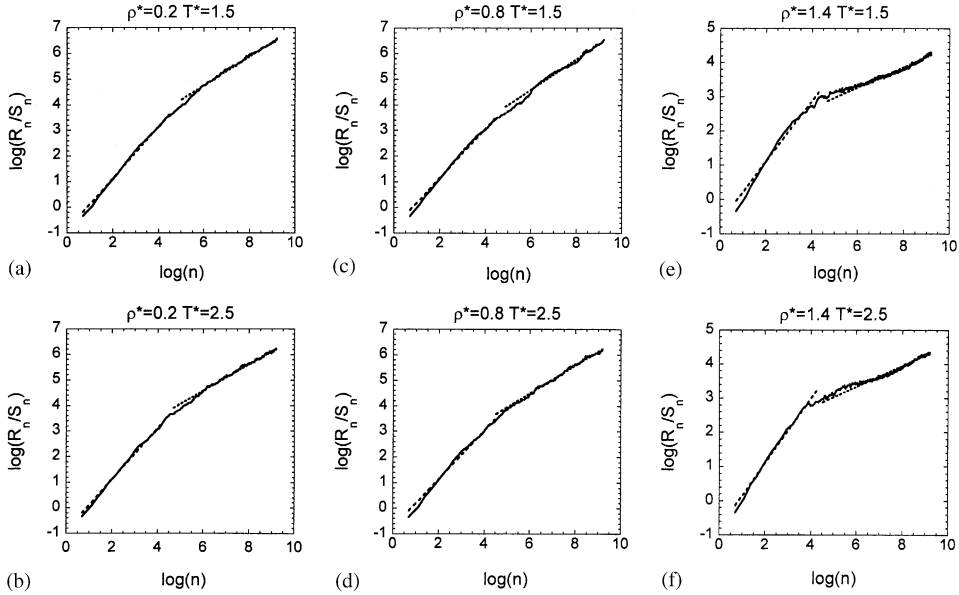

Fig. 8. Hurst test results for the pressure time series at various system densities ρ^* and temperatures T^*.

with the power spectrum results of Section 3.1. R/S analysis results for the potential energy are identical, within numerical accuracy, to those of the kinetic energy (temperature) (for reasons explained in Section 3.1) and thus Hurst exponents for the potential energy are not presented.

In Fig. 8 we present representative R/S analysis results for the instantaneous pressure time series. We clearly observe that we again have a two-regime behaviour: a linear type behaviour for small n (small time intervals) and a linear behaviour with a smaller slope for higher n (large time intervals). We calculated the slopes and the corresponding Hurst exponents for both regions and summarized the results for all simulated states in Fig. 9. We observe that for small n (small time intervals) H is close to 1.0 indicating strong persistence, i.e., new values follow the trend of previous ones, which is in agreement with the spectral analysis results. For large n (large time intervals) H is in general smaller than 0.7 and seems to take values close to 0.5 as the temperature increases. The reduction in the value of H seems to be faster than for temperature (and naturally potential energy). This behaviour indicates that memory is very quickly lost at small frequencies as it was observed in the spectral analysis presented in Section 3.1.

In the solid phase, the exponent H for small n shows a behaviour similar to that of the fluid, in accordance with the result of high-frequency spectral analysis where we have strong memory effects. For large n (small frequencies) the exponents are smaller, around 0.3–0.5, indicating a very fast loss of memory in agreement with the power spectrum results.

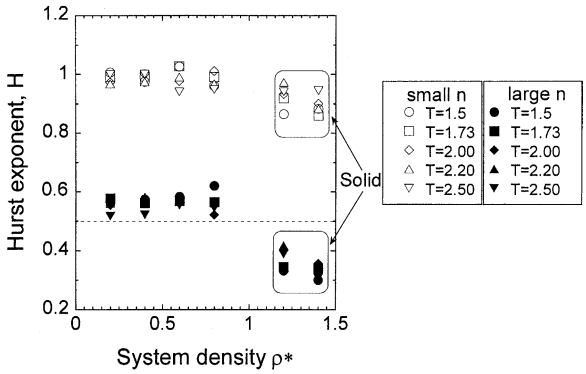

Fig. 9. Hurst exponents for the pressure time series as a function of system temperature and density.

3.3. Mean square displacement

Among physical quantities that reflect the intrinsic dynamics of a system of particles is the mean square displacement (MSD) which is a correlation function defined by

$$\delta r^2(t) = \frac{1}{N}\sum_{i=1}^{N}[\vec{r}(0) - \vec{r}(t)]^2 \ . \tag{12}$$

MSD shows how far a particle can reach from its original position after a given time t.

We have calculated the MSD for all system densities and temperatures studied in order to see if the results are in agreement with the findings from the time series analysis and if there is any relation with characteristic times deduced from the power spectrum analysis presented in Section 3.1. As expected, for the fluid as the system density increases MSD decreases since increasing density results in less available space for atoms to move. In fact for low densities atoms diffuse very easily spending a short time oscillating at given residence sites while at higher densities atoms are more confined and thus they spend more time oscillating around sites of residence before diffusing. This can be seen in Figs. 10(a)–(b) which show typical trajectories of atoms of the fluid for $T^* = 1.5$ at the lowest ($\rho^* = 0.2$) and the highest ($\rho^* = 0.8$) density. We can see that at high densities (Fig. 10(b)) atoms are for some time localized at a given space region while at lower densities (Fig. 10(a)) they are far less localized and as a result they travel longer distances leading to higher MSD at low densities. This behaviour also means that at high densities we have a faster loss of memory and this will hold for the velocities and temperature as we have seen from the power spectrum and Hurst analysis in the previous sections.

In the solid phase, atoms vibrate around their positions resulting in MSD that increases parabolically for very short time intervals in a way similar to that of the fluid and then fluctuates around a given value that is related to the amplitude of vibration of the atoms. The former behaviour is indicative of strong memory effects at short times while the latter is indicative of loss of memory at large times. Recall that

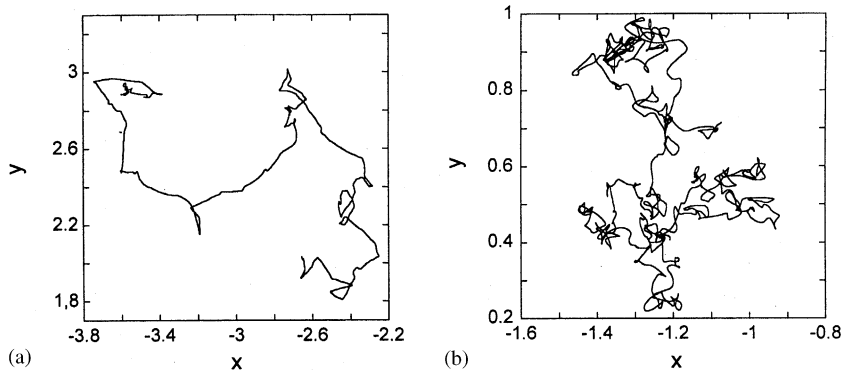

Fig. 10. Typical trajectories of atoms (projection on x–y plane) at (a) $T^* = 1.5$ and $\rho^* = 0.2$, (b) $T^* = 1.5$ and $\rho^* = 0.8$.

both potential energy which depends directly on positions (Eq. (3)) and temperature which depends on velocities (Eq. (2)), (i.e., derivatives of the positions) exhibit strong memory effects for small times and loss of memory at large times. Thus the MSD results are in general agreement with the results presented in Section 3.1.

It is of interest to examine the asymptotic behaviour of the MSD for very short times. For short times we have a parabolic dependence on time, practically the same for all fluid densities, as it is expected [25]. This is also in agreement with the computed power spectra where for high frequencies we found that the value of the exponent a is insensitive to the variation of the system density. An analogous behaviour is observed for the solid states but the similarity region extends over a smaller time interval which means that it corresponds to higher frequencies. The reader is reminded here that the high-frequency power-law behaviour for the solid is observed at higher frequencies than in the fluid. It is interesting to note that the maximum time that this behaviour is observed for the fluid states is around 2×10^{-13} s which corresponds to a frequency of about 5×10^{12} Hz which, in turn, is the lower limit of the high-frequency zone in the power spectra (Figs. 2(a) and (b) and 4(a) and (b)). For the solid, as the corresponding maximum time is smaller, around 1.5×10^{-13} s, we find a frequency around 8×10^{12} Hz which is the lower limit of the high-frequency regime in the power spectra (see Figs. 2(c) and (d) and 4(c) and (d)).

4. Conclusions

In this work we have performed the simulation of fluid and solid states of argon using a Lennard–Jones potential to describe atomic interactions. For all the simulated states we performed an analysis of the time series of instantaneous temperature, potential energy and pressure. The time series were obtained at densities varying from 0.2 up to 1.4 and reduced temperatures T^* in the range [1.5–2.5].

Spectral analysis indicates a two-regime power-law behaviour for all time series, the exponents being different in the two regimes. For temperature we have a high-frequency regime with a large exponent indicating strong memory effects and a low-frequency regime where the power-law exponent is smaller indicating rapid loss of memory. For high frequencies, pressure behaves similarly. In contrast, at low frequencies, pressure is characterized by exponents close to zero indicating a faster loss of memory. The high-frequency exponents for all physical quantities studied are insensitive to the density variation while the low-frequency exponents become smaller as density increases. As the system temperature increases the values of the power spectrum exponents are in general smaller indicating that increasing temperature weakens memory effects.

Hurst analysis also shows a two-regime behaviour consistent with the results obtained from spectral analysis. At small time intervals we have strong persistence and at long times memory is rapidly lost. Pressure loses memory faster than the temperature (and potential energy) at long time intervals.

The mean square displacement results seem to confirm the analysis and the characteristic times based on MSD calculation are found to be in agreement with the characteristic times extracted from the spectral and Hurst analyses of the temperature and pressure time-series.

It is of interest that the characteristic times of the system can be extracted from the power spectrum behaviour of the studied time series and that several dynamic characteristics of the physical system are reflected in both microscopic (potential energy) and macroscopic quantities (temperature, pressure).

Acknowledgements

T.E. Karakasidis wishes to thank the Greek State Scholarship Foundation (IKY) for partial support of this work under a postdoctoral research Grant No. 312/2001.

References

[1] A.R. Bizzarri, S. Cannistraro, Physica A 267 (1999) 257.
[2] A. Bulgac, Z. Phys. D 40 (1997) 454.
[3] T.E. Karakasidis, I. Andreadis, Chaos, Solitons and Fractals 15 (2003) 87.
[4] V.M. Vritsky, M.I. Pudovkin, Ann. Geophys. 16 (1998) 1580.
[5] W.H. Press, Comm. Astron. 7 (1978) 103.
[6] M.J. Kirton, M.J. Uren, Adv. Phys. 38 (1989) 367.
[7] M.B. Weissman, Rev. Mod. Phys. 60 (1988) 537.
[8] M.B. Weissman, Rev. Mod. Phys. 65 (1993) 829.
[9] I. Andreadis, Chaos, Solitons and Fractals 11 (2000) 1047.
[10] I. Andreadis, A. Serletis, Int. J. Syst. Sci. 2 (2001) 43.
[11] B.J. West, M.F. Shlesinger, Int. J. Mod. Phys. B 3 (1989) 795.
[12] L. Verlet, Phys. Rev. 159 (1967) 98.
[13] L. Verlet, Phys. Rev. 165 (1968) 201.
[14] D. Levesque, L. Verlet, J. Kurkijarvi, Phys. Rev. A 7 (1973) 1690.
[15] D.M. Heyes, J. Chem. Soc. Faraday Trans. 80 (1984) 1363.
[16] F.F. Abraham, J. Mech. Phys. Solids 49 (2001) 20951.

[17] F.F. Abraham, R. Walkup, H.J. Gao, M. Duchaineau, T.D. De la Rubia, M. Seager, Proc. Natl. Acad. Sci. USA 99 (2002) 5777.
[18] T.E. Karakasidis, A.B. Liakopoulos, Technical Report 2002—01, Hydromechanics Laboratory, University of Thessaly, 2002.
[19] W. Li, Int. J. Bifurcation Chaos 1 (1991) 583.
[20] A. Rahman, J. Chem. Phys. 45 (1966) 2585.
[21] J.L. Lebowitz, J.K. Percus, L. Verlet, Phys. Rev. 153 (1967) 250.
[22] B.B. Mandelbrot, The Fractal Geometry of Nature, Freeman, San Francisco, 1982.
[23] B.B. Mandelbrot, Gaussian, Self-Affinity and Fractals, Springer, Berlin, 2001.
[24] J.G.V. Miranda, R.F.S. Andrade, Theoret. Appl. Climatol. 63 (1999) 79.
[25] F. Kohler, The Liquid State, Verlag Chemie, Weinheim, 1972.